

Performance of cyclic injections in soft granular media: Trapping efficiency and hysteretic behaviour

Haiyi Zhong¹, Zhongzheng Wang², Si Suo³ and Yixiang Gan¹

¹ School of Civil Engineering, The University of Sydney, NSW 2006, Australia

² School of Mechanical, Medical and Process Engineering, Faculty of Engineering, Queensland University of Technology, QLD 4001, Australia

³ Department of Civil and Environmental Engineering, Imperial Collage London, London, SW7 2AZ, United Kingdom.

Abstract: Carbon dioxide (CO₂) and hydrogen (H₂) storage in geological formations are two key approaches to reducing carbon emissions, with capillary trapping serving as one of the primary trapping mechanisms. Understanding the behaviour of immiscible fluid-fluid displacement in porous media is crucial for optimizing trapping efficiency. However, previous studies have primarily focused on single injection scenarios in non-deformable particles, with limited attention given to cyclic scenarios and conditions where the porous media may deform under injection-induced stress. To address this gap, this study experimentally investigates the effects of solid deformability (*i.e.*, hard and soft particles) on trapping behaviours during single and cyclic injections under quasi-2D conditions using a Hele-Shaw cell. In soft media, gas bubbles evolve from cavities to small blobs during cyclic injections, leading to a noticeable increase in residual saturation compared to single injection. In contrast, hard granular media exhibit pore invasion from the onset, with residual saturation remaining independent of the number of injection cycles. These findings demonstrate that solid deformability plays a critical role in governing the dependence of residual trapping on injection schemes. These insights offer valuable guidance for developing more effective and optimized strategies for geological gas storage.

1 Introduction

Reducing high carbon dioxide (CO₂) emissions has become increasingly urgent to mitigate the adverse impacts of climate change [1]. Two of the most significant approaches to address this issue are carbon capture and storage (CCS) and renewable energy systems, with hydrogen (H₂) often serving as an energy carrier to ensure the stable energy supply in the latter [2]. Currently, geological formations, typically composed of porous media, are considered one of the most effective and practical options for gas storage owing to their wide availability [3]. In these storage media, capillary trapping is a key trapping mechanism. For permanent CO₂ storage, it is recognised as the most efficient method for ensuring storage security [4]. However, as H₂ needs to be withdrawn for use, this mechanism will adversely affect the energy efficiency. Therefore, understanding how capillary trapping influences the behaviour of immiscible fluid-fluid displacement in porous media is crucial for optimizing storage and production strategies.

Many experimental studies have focused on a single drainage-imbibition cycle [5]. However, in real-world field applications, both CO₂ and H₂ are often subjected to cyclic injections. Relatively few studies have examined sequential drainage-imbibition cycles, and the effects of these cycles on trapping efficiency remain inconsistent. Some studies suggest that gas residual saturation evolves over successive injection cycles [6-8],

while others report no significant change over time [9,10]. Apart from the limited studies on cyclic injections, previous research has largely overlooked the effects of solid deformability, focusing primarily on trapping behaviours in geometrically fixed and rigid porous media [6,11]. However, recent experimental study indicates that the pore volume ratio of sandstone increases with both the number of injection cycles and rising pore pressure [12]. This suggests that in real-world scenarios where pressure conditions can vary significantly from 1 MPa to over 30 MPa, storage media at the pore scale can range from relatively rigid solids to deformable material. Fluid injection into a deformable medium can induce deformation and displacement of the host solids, which in turn influences overall trapping behaviours. Recently, only a few studies have explored gas injection in soft porous media [13,14]. While these studies primarily examine solid deformation or injected flow patterns during single injections, there is a significant gap in understanding gas transport and trapping behaviours during cyclic injections in deformable porous media.

To address these gaps, this study carried out experimental tests using vertical Hele-Shaw cells containing a quasi-2D monolayer particles, which allows for clear visualization and quantitative analysis of the trapped gas. It aims to study the effects of solid deformability (*i.e.*, soft and hard particles) and injection regimes (*i.e.*, single and cyclic injections) on trapping behaviours. With the experimental design and analyses

of the results, we focus on improving our understanding of the interplay between solid deformability and injection regimes to optimise trapping/withdraw efficiency and storage security.

2 Experimental system

2.1 Test materials

In this study, silicone spheres and polyacrylamide hydrogel (JRM Chemical) were used to assemble granular media with distinct mechanical properties, as shown in Fig. 1 (a). The silicone spheres have an estimated Young's modulus of ~ 735 kPa [15], while the hydrogel particles have a Young's modulus of approximately ~ 10 kPa [13]. The silicone spheres were fabricated to a target size of 2 ± 0.1 mm through a precise moulding process. For the hydrogel, it was initially in powdered form and swelled into soft grains upon mixing with water. Since the raw material originally comprised grains of varying sizes, a sieve analysis was conducted to ensure size consistency with the silicone spheres. Dry grains with a size range of 0.25-0.3 mm were selected. After 24 hours of saturation in demineralized water, the swollen hydrogel grains expanded to a size range of 1.7-2.1 mm. To further enhance uniformity, the swollen hydrogel grains were sieved using customized 3D-printed sieves with openings of 1.9 mm and 2.1 mm.

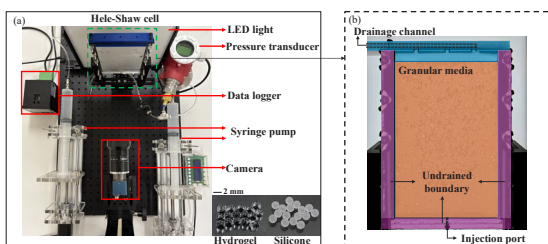


Fig. 1 (a) Overview of the custom-developed test setup (top view) and test materials; (b) Boundary conditions of 2D Hele-Shaw cell.

2.2 Test setup

A custom-developed system was employed to investigate the gas-liquid displacement in porous media, as shown in Fig. 1 (a). The entire experimental setup was mounted on an optical platform (flatness: ± 0.05 mm over 0.36 m²) to ensure a uniform surface, with all components aligned at the same absolute height. The system includes a visualization Hele-Shaw cell, two syringe pumps (Y.H. POWER, QHLR-0140), an industrial digital camera (DAHENG, MER2-2000-19U3M), a pressure transducer (MEACON, SUP-P3-000D), a data logger (MEACON, MIK-RN 3000) and a LED light (JSIONX, JS-DBL209-318). The visualization cell (Fig. 1 (b)) was constructed from two transparent acrylic sheets (120 mm \times 160 mm \times 7.5 mm) separated by acrylic strips (10 mm \times 160 mm \times 1.5 mm) positioned on both sides. These strips were lined with Ethylene Propylene Diene Monomer (EPDM) foam strips of 1 mm thickness. This configuration allows the gap between the two acrylic sheets to be adjusted to

2.15 ± 0.02 mm, enabling the formation of a quasi-2D monolayer of particles. Additionally, these strips also effectively prevented liquid leakage from the cell. The top of the cell was equipped with a 3D-printed module with an internal channel connected to the cell to facilitate drainage and gas escape. The bottom of the cell was secured with an acrylic strip containing an injection port, which was connected to syringe pumps via plastic tubing. After assembling the Hele-Shaw cell, the edges were sealed with glass glue to prevent any unintended gas or liquid leakage.

2.3 Test procedures

After saturating the Hele-Shaw cell with deaired water, the particles were packed in monolayer. The desired packing height for all cases was consistent. Once the packing phase was completed, 3D-printed modules were fixed on top. The remaining particles were then weighted again to accurately calculate the porosity. The assembled cell was then mounted on the platform in front of the LED light and the bottom injection port was connected to two syringe pumps. Two injection schemes were employed: single and cyclic injections, both conducted at a constant injection rate of $Q = 3$ ml/minute. The single injection process includes 20-min air injection followed by 20-min water injection. In the cyclic injection scheme, four imbibition-drainage cycles were performed, each consisting of 5 minutes of air injection followed by 5 minutes of water injection. The gas migration pattern was recorded during the entire process at 4 frames per second with a high resolution of $5,496 \times 3,672$ pixels. Four sets of experiments were conducted with varying materials, injection schemes and porosities, as summarized in Table 1.

Table 1 Summary of test conditions

Test ID ^a	Test material	Porosity	Injection scheme ^b
H-S	Silicone	0.346 ± 0.017	Single
H-C	(Hard)		Cyclic
S-S	Hydrogel	0.341 ± 0.027	Single
S-C	(Soft)	0.344 ± 0.027	Cyclic

Notes:

^a This first symbol denotes the test material type: 'H' for hard and 'S' for soft; the second symbol indicates the injection scheme: 'S' for single injection and 'C' for cyclic injections.

^b Single injection contains 20-min air injection and 20-min water injection; cyclic injections include 4 cycles of 5-min air and 5-min water injections

3 Results

3.1 Dynamic evolution of trapped gas

To visualize the effects of injection regimes on trapping behaviour, we compare fluid displacement patterns and residual saturation at the steady state. The invading gas phase was categorized into different sizes, represented by a colour gradient from small (0 mm², blue) to large (250 mm², red).

For soft granular media, cyclic injections (Test S-C) resulted in a distinct evolution, as shown in Fig. 2 (a). This evolution is characterized by a significant increase in gas residual saturation, rising from 0.04 to 0.40, along

with clusters transiting from cavities to interconnected ganglia and eventually forming predominantly blobs that dominating the system. Compared to the single injection results (Test S-S), a similar outcome is observed, with small ganglia dominating in the final state. However, the terminal residual saturation is approximately three times lower (0.12). This discrepancy aligns with studies suggesting that gas residual saturation evolves over successive injection cycles [6-8].

The trapping behaviour of hard granular media (Test H-S and H-C) is shown in Fig. 2 (b). The cluster size is noticeably smaller than that in the soft case. Since the hard particles are almost non-deformable in this experimental setting, this rigidity limits the mobility of the gas phase and the potential for cluster coalescence and redistribution. The residual saturation stabilizes after cycle 2, which is faster than the soft case. Interestingly, the residual saturation across different injection regimes is similar. This observation is consistent with studies suggesting that residual saturation during cyclic injections remains constant over time [9,10].

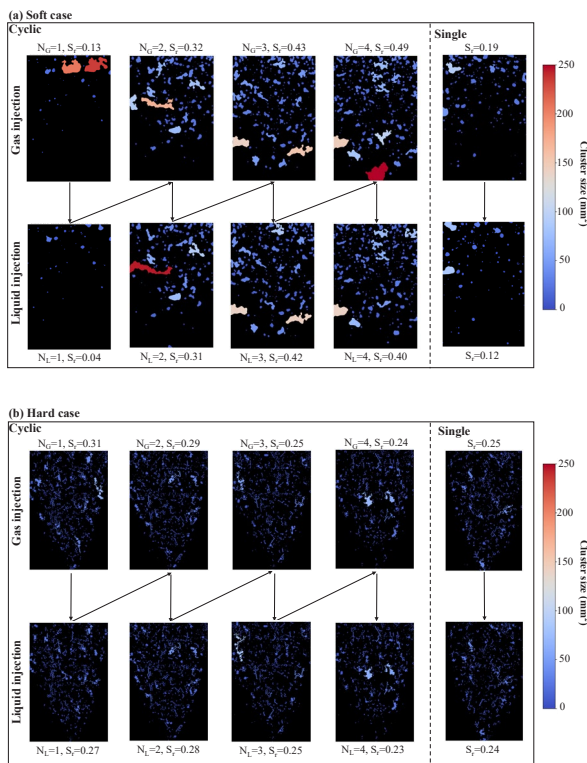


Fig. 2 Comparisons of migration patterns at steady state (NG and NL represents the number of gas and liquid injection) (a) Soft granular media (Test S-C and S-S); (b) Hard granular media (Test H-C and H-S).

3.2 Hysteresis effects of cyclic injections

To quantify the hysteresis effects during cyclic injections, the initial and residual gas saturations for each cycle are plotted in Fig. 3, alongside data from recent representative experimental studies on cyclic injections [7,11,17] for comparison. The data in this study represent average values from the final minute of each drainage/imbibition process, with measurements

recorded every five seconds. The gradient colour from dark to light indicates the cycle sequence. The results are compared with the classic trapping model proposed by [18], represented by black solid curves:

$$S_{r,G} = \frac{S_{i,G}}{1 + C \cdot S_{i,G}}, \quad (1)$$

where $S_{i,G}$ and $S_{r,G}$ represent the residual saturation after imbibition and drainage upon reaching the steady state, respectively; C is the Land trapping coefficient. These trajectories represent the evolution of saturation hysteresis throughout the cyclic injections. In general, neither the trajectories from this study nor those from the literature strictly follow the trend predicted by Land model, indicating that relying solely on this model may not adequately capture gas hysteresis behaviours during cyclic injections. For the hard case (Test H-C), the trajectory across all cycles remains nearly fixed at a value close to the Land model curve with $C=0.4$ and shows no clear trend, resembling the reported experimental results [11,16]. Focusing on soft case (Test S-C), the observed phenomenon is similar to the previous findings [7,17]. A notable feature in these cases is the trend of trajectories moving in a direction of decreasing C, which is associated with smaller changes in saturation after water flooding. It is worth noting that the studies [11,16], which produced results comparable to those for hard granular media, were conducted under ambient pressure. In contrast, the studies [7,17], which exhibited behaviours similar to soft granular media, were conducted under MPa-level pore pressure. This suggests that high pressure may increase the pore-scale deformability of rock samples, allowing the injected fluid to alter the pore size and causing the material to behave more like soft media. This behaviour has been also demonstrated in previous experiments [12].

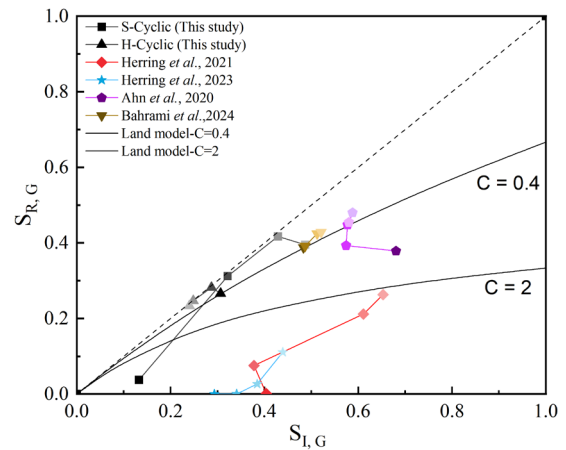


Fig. 3 Trajectories of initial and residual gas saturation during cyclic injections with varying solid deformability and injection schemes. The gradient colour from dark to light indicates the cycle sequence.

4 Conclusions

This study experimentally investigated the effects of solid deformability and injection schemes (*i.e.*, single and cyclic injections) on gas trapping behaviours in a vertical Hele-Shaw cell. Contrasting solid deformability can lead to significantly different trapping behaviours.

In the soft case, trapped gas evolves from large cavities into interconnected ganglia and eventually forms predominantly blobs over successive cycles, notably enhancing residual gas saturation. Whereas the hard case exhibits pore invasion from the onset, with residual saturation remaining nearly unchanged throughout the cycles. Compared to single injection, cyclic injections significantly enhance gas retention in the soft case, whereas residual saturation in the hard case remains similar across both injection scenarios. The evolution of residual saturation during cyclic injections is compared with the predictions of Land model, revealing that relying solely on this model may not adequately capture hysteresis effects. In hard granular media, no clear trend is observed, which is consistent with the experimental findings conducted under ambient pressure. In contrast, soft granular media clearly shows enhanced trapping efficiency, resembling the behaviour observed in tests conducted under MPa-level pore pressure. This indicates that the previous inconsistent conclusions (either no change or evolve) regarding the cyclic injection effects could possibly relate to the relative deformability of storage media.

References

1. A. Raza, R. Gholami, R. Rezaee, V. Rasouli, M. Rabiei, Significant aspects of carbon capture and storage-A review. *Petroleum* **5**, 4 (2019). <https://doi.org/10.1016/j.petlm.2018.12.007>
2. H. Zhong, Z. Wang, Y. Zhang, S. Suo, Y. Hong, L. Wang, Y. Gan, Gas storage in geological formations: A comparative review on carbon dioxide and hydrogen storage. *Mater. Today Sustain.* **26**, (2024). <https://doi.org/10.1016/j.mtsust.2024.100720L>.
3. S. Niaz, T. Manzoor, A.H. Pandith, Hydrogen storage: Materials, methods and perspectives. *Renew. Sust. Energ. Rev.* **50**, (2015). <https://doi.org/10.1016/j.rser.2015.05.011>
4. A. Raza, R. Rezaee, C.H. Bing, R. Gholami, M.A., Hamid, R. Nagarajan, Carbon dioxide storage in subsurface geologic medium: A review on capillary trapping mechanism. *Egyptian Journal of Petroleum*, **25**, 3 (2016). <https://doi.org/10.1016/j.ejpe.2015.08.002>
5. R.M. El-Maghraby, M.J. Blunt, Residual CO₂ trapping in Indiana limestone. *Environ. Sci. Technol.* **47**, 1 (2013). <https://doi.org/10.1021/es304166u>.
6. A.L. Herring, L. Andersson, D. Wildenschild, Enhancing residual trapping of supercritical CO₂ via cyclic injections. *Geophys. Res. Lett.* **43**,18 (2016). <https://doi.org/10.1002/2016GL070304>
7. A.L. Herring, C. Sun, R.T. Armstrong, Z. Li, J.E. McClure, M. Saadatfar, Evolution of Bentheimer Sandstone Wettability During Cyclic scCO₂-Brine Injections. *Water Resour. Res.* **57**, 11 (2021). <https://doi.org/10.1029/2021WR030891>
8. Z. Wang, J.M. Pereira, E. Sauret, Y. Gan, Wettability impacts residual trapping of immiscible fluids during cyclic injection. *J. Fluid Mech.* **961**, (2023). <https://doi.org/10.1017/jfm.2023.222>
9. A. Saeedi, R. Rezaee, Effect of residual natural gas saturation on multiphase flow behavior during CO₂ geo-sequestration in depleted natural gas reservoirs. *J. Petrol. Sci. Eng.* **82-83**, (2012). <https://doi.org/10.1016/j.petrol.2011.12.012>
10. C. Garing, S.M. Benson, CO₂ Wettability of Sandstones: Addressing Conflicting Capillary Behaviors. *Geophys. Res. Lett.* **46**, 2 (2019). <http://dx.doi.org/10.1029/2018GL081359>
11. H. Ahn, S.O. Kim, M. Lee, S. Wang, Migration and Residual Trapping of Immiscible Fluids during Cyclic Injection: Pore-Scale Observation and Quantitative Analysis. *Geofluids* **1**, (2020). <https://doi.org/10.1155/2020/4569208>
12. X. Qiu, H. Liu, M. Liu, H. Mao, D. Wang, Q. Ying, S. Ban, Pore structure evolution in sandstone of underground gas storage during cyclic injection and production based on nuclear magnetic resonance technology. *Energies* **16**, 5, (2023). <https://doi.org/10.3390/en16052096>
13. S. Lee, J. Lee, R. Le Mestre, F. Xu, C.W. MacMinn, Migration, trapping, and venting of gas in a soft granular material. *Phys. Rev. Fluids* **5**, 8 (2020). <https://doi.org/10.1103/PhysRevFluids.5.084307>
14. A.H. Zadeh, M.K. Jeon, T.H. Kwon, S. Kim, Pore-scale experimental study on fluid injection into two-dimensional deformable porous media. *Int. J. Multiph. Flow* **160**, (2023). <https://doi.org/10.1016/j.ijmultiphaseflow.2022.104376>
15. I.M. Meththananda, S. Parker, M.P. Patel, M. Braden, The relationship between Shore hardness of elastomeric dental materials and Young's modulus. *Dent. Mater.* **25**, 8 (2009). <https://doi.org/10.1016/j.dental.2009.02.001>
16. M. Bahrami, H. Mahani, D. Zivar, S. Ayatollahi, Microfluidic investigation of pore-scale flow behavior and hysteresis in underground hydrogen storage in sandstones. *J. Energy Storage*, **98**, (2024). <https://doi.org/10.1016/j.est.2024.112959>
17. A.L. Herring, C. Sun, R. Armstrong, M. Saadatfar, Insights into wettability alteration during cyclic scCO₂-brine injections in a layered Bentheimer sandstone. *Int. J. Greenh. Gas Control* **122** (2023). <https://doi.org/10.1016/j.ijggc.2022.103803>
18. C. S. Land, Calculation of imbibition relative permeability for two-and three-phase flow from rock properties. *Soc. Petrol. Eng. J.* **8**, 2 (1968).